Evidence for Electron Acceleration up to ~300 keV in the Magnetic Reconnection Diffusion Region of Earth's Magnetotail

M. Øieroset, R. P. Lin, T. D. Phan, D. E. Larson, and S. D. Bale

Space Sciences Laboratory, University of California, Berkeley, California 94720

(Received 28 June 2002; published 18 October 2002)

We report direct measurements of high-energy particles in a rare crossing of the diffusion region in Earth's magnetotail by the Wind spacecraft. The fluxes of energetic electrons up to ~300 keV peak near the center of the diffusion region and decrease monotonically away from this region. The diffusion region electron flux spectrum obeys a power law with an index of −3.8 above ~2 keV, and the electron angular distribution displays strong field-aligned bidirectional anisotropy at energies below ~2 keV, becoming isotropic above ~6 keV. These observations indicate significant electron acceleration inside the diffusion region. Ions show no such energization.

DOI: 10.1103/PhysRevLett.89.195001 PACS numbers: 52.20.-j, 52.30.Ex, 52.50.-b, 94.30.Ej

Magnetic reconnection is a universal plasma process which converts stored magnetic energy into kinetic energy in the form of fast flows, heating, and particle acceleration [1]. It was first proposed as a mechanism for the release of energy in solar flares [2], but is also thought to be important in other astrophysical contexts. The process involves the breaking and change of magnetic connectivity in a localized region, the so-called diffusion region [3]. Recent soft x-ray and extreme-ultraviolet imaging observations provide strong evidence that reconnection is indeed occurring in solar flares [4,5], while hard x-ray observations indicate that a large fraction (~ 10%–50%) of the total energy released is contained in accelerated ~10–100 keV electrons [6,7]. Reconnection is also known to operate at Earth's magnetopause [8] and in the magnetotail [9,10] allowing solar wind plasma to enter the magnetosphere. Fast, bidirectional plasma jets consistent with reconnection predictions have been detected at the magnetopause [8,11–13] and in the magnetotail [14,15]. Bursts of energetic $\gtrsim 200$ keV electrons detected in the magnetotail have also been attributed to reconnection [16–18]. However, little is known about how energetic particles are accelerated and where; whether within the diffusion region directly by the reconnection process itself or whether they are the by-product of reconnection, generated in the outflow region outside the diffusion region [19].

Until now, no observations of high-energy particles in the diffusion region have been reported, due to the scarcity of diffusion region encounters [20–22]. In this Letter, we report the first measurements of high-energy particles inside the diffusion region, in a fortuitous crossing by the Wind spacecraft in the distant magnetotail, 60 Earth radii behind Earth [20]. We find that (i) the most intense high-energy electron fluxes and the hardest energy spectrum occur in the diffusion region, with a monotonic decrease in fluxes and softening of the energy spectrum on either side, and (ii) the ions do not show such energization in the diffusion region.

Figure 1 shows Wind measurements in and around the ion diffusion region for the 06:30–10:00 UT interval on 1 April 1999, from the 3D plasma and energetic particle experiment [23] and the magnetometer experiment [24]. The diffusion region crossing lasted 19 min and is marked with the red horizontal bar in Fig. 1(b). This region was identified by Øieroset *et al.* [20] based on (i) an uninterrupted transition from earthward to tailward plasma jets without leaving the reconnection layer [Fig. 1(b)]; (ii) quadrupolar Hall magnetic field signatures signifying the decoupling of ions from electrons expected in the ion diffusion region [20]; (iii) an electron beam with direction consistent with being the Hall current carrier [20]. The basic reconnection configuration, the coordinate system, and the spacecraft trajectory are described in Fig. 2. During the 3.5 h interval shown in Fig. 1, the spacecraft stayed mainly in the high density ($\sim 0.1\ \mathrm{cm}^{-3}$) plasma sheet with occasional excursions into the lower density ($< 0.03\ \mathrm{cm}^{-3}$) lobe region [Fig. 1(a)]. High speed plasma jets along the earthward (positive x) or tailward (negative x) direction were observed whenever Wind was in the plasma sheet [Fig. 1(b)] indicating that reconnection was quasicontinuous for many hours. The location of the flow reversal (from earthward to tailward direction) at 07:56 UT defines the center of the diffusion region along x although this location may be offset from the true center in the z direction (see Fig. 2). The x component of the magnetic field provides an indication of the location of the spacecraft relative to the magnetotail neutral sheet [Fig. 1(c)]. A large B_x implies high magnetic latitude observations, away from the neutral sheet. Both the electron and ion temperature [Figs. 1(d) and 1(e)] exhibited an abrupt increase as the spacecraft went from the earthward to the tailward side of the X line at 07:56 UT.

Figures 1(f) and 1(g) show the electron phase space densities for energies between 4 and 300 keV. The high-energy phase space density up to 300 keV exhibits a distinct maximum near the center of the diffusion region

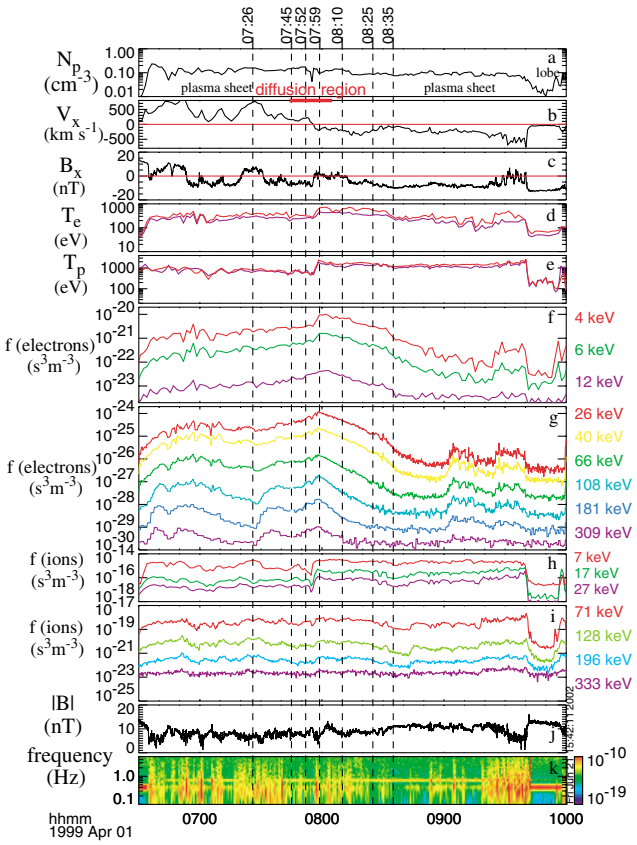

FIG. 1 (color). Plasma, energetic particles, and magnetic field observations inside and outside the ion diffusion region for the 06:30–10:00 UT interval on 1 April 1999, from the Wind spacecraft. The diffusion region is marked with the red horizontal bar. (a) Plasma density; (b) plasma velocity along x (see Fig. 2 for definition of coordinate system); (c) x component of the magnetic field; (d) electron parallel (red) and perpendicular (blue) temperature; (e) ion parallel (red) and perpendicular (blue) temperature; (f),(g) electron phase space density from 4 to 300 keV; (h),(i) ion phase space density from 7 to 300 keV; (j) magnetic field magnitude; (k) magnetic field wave power for frequency less than 4 Hz. Higher frequency wave data from the wave experiment are not available for this event. The vertical dashed lines mark the times of the particle distributions plotted in Fig. 3. Full 3D high-energy particle observations are made every 12 sec by semiconductor telescopes measuring 20–500 keV electrons and 30 keV–6 MeV ions [23]. 3D measurements of the thermal and suprathermal plasma below 30 keV are obtained from electrostatic analyzers measuring ions with energies between 80 eV and 30 keV and electrons with energies from a few eV to 30 keV with time resolution varying between 50 and 96 sec [23]. The magnetic field magnitude and direction are sampled 10 times per second [24].

[Fig. 1(b)]. The high-energy (70–300 keV) ion flux, on the other hand, does not show such an enhancement in the diffusion region [Figs. 1(h) and 1(i)].

Figures 3(a) and 3(b) show the evolution of the electron distribution as one approaches the center of the diffusion region from the earthward and tailward side, respectively.

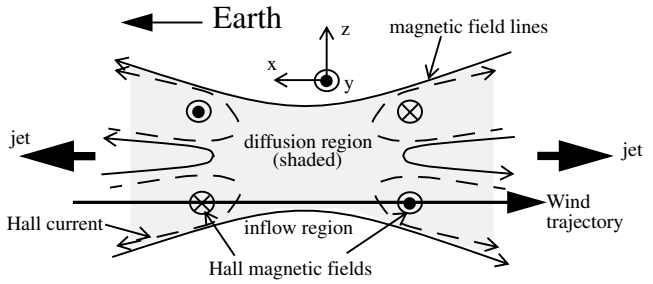

FIG. 2. Schematics of the magnetic reconnection diffusion region. Oppositely directed magnetic field lines convect toward each other from the top and the bottom of the figure and reconnect at an X point or X line. Magnetic energy is converted into kinetic energy in the form of bidirectional plasma jets. In the ion diffusion region, marked by the shaded area, the separation of ions and electrons creates a system of Hall currents and associated Hall magnetic fields [30], which were observed by the Wind spacecraft [20]. The Wind trajectory through the diffusion region from the earthward to the tailward side is marked on the plot. The coordinate system is defined such that x points towards the Sun (and Earth), z is normal to the current sheet, and y is directed out of the plane.

A Maxwellian distribution with a plasma density of 0.1 cm^{-3} and an electron temperature of 400 eV is plotted with the dash-dotted line for comparison. The observed electron distributions deviate significantly from a Maxwellian distribution above ~2 keV. The straight dashed lines in Figs. 3(a) and 3(b) show the least square fits of the high-energy parts of the electron distributions to a power law distribution, $f \propto E^{-k}$. The power k varies from 5.7 away from the diffusion region to 4.8 near the center of the diffusion region. When fitted to differential flux spectra instead, we obtain $dJ/dE \propto E^{-3.8}$ near the center of the diffusion region and $dJ/dE \propto E^{-4.7}$ away. Thus, the spectrum gradually becomes harder (i.e., more energetic) towards the center of the diffusion region.

The corresponding ion distributions also exhibit extended high-energy tails [Fig. 3(c)], but the fluxes and the slope of the distribution stay relatively constant as the spacecraft moves away from the diffusion region [as is apparent also from Fig. 1(i)]. A Maxwellian distribution with an ion temperature of 1500 eV, a plasma density of 0.1 cm^{-3}, and a plasma velocity of 200 km s^{-1} is plotted with the dash-dotted line for comparison and is a good approximation for energies up to ~10 keV.

The pitch-angle distribution of the electrons also changes as the spacecraft moves across the diffusion region. On the earthward side of the X line outside the diffusion region, we find a near-isotropic distribution at all energies [Fig. 4(a)]. When the high-energy phase space density reaches its maximum, near the center of the diffusion region, the distributions at energies from 15.2 eV to ~1 keV (i.e., the Maxwellian portion) display peaks at 0° and 180° and minima at 90° [Fig. 4(b)]. In the intermediate energy range (from 1 to 6 keV), the minima

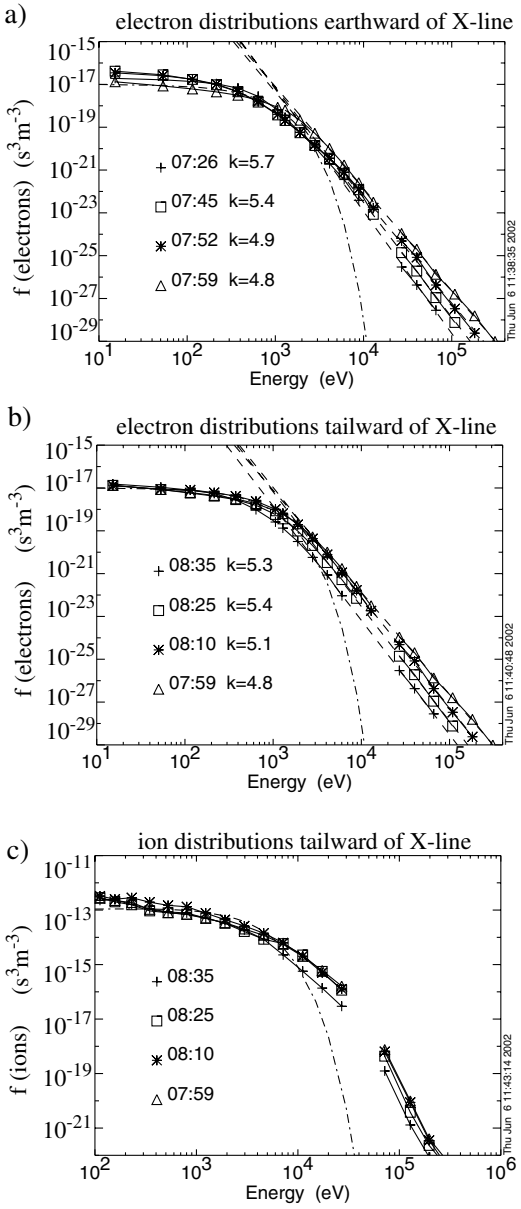

FIG. 3. (a) Electron distribution function on the earthward side of the X line; (b) electron distributions on the tailward side; (c) ion distributions on the tailward side. The statistical error in the particle measurements is less than 5% and therefore not plotted. The times of the distribution measurements are marked with vertical dashed lines in Fig. 1. The power law index k for the least square fits (dashed lines) are indicated in the plots. If differential flux spectra instead of distribution function were fitted, k would vary from 4.7 outside the diffusion region to 3.8 at the center of the diffusion region.

at 90° are still apparent but the distributions flatten out near 0° and 180°. At higher energies (> 6 keV), the electrons become nearly isotropic. This type of gradual evolution of distribution from field-aligned counterstreaming to isotropy with increasing energy is most pronounced for electrons detected in the diffusion region. On the tailward side of the X line [Fig. 4(c)], the pitch-angle spectrum becomes much more isotropic again for almost all energies.

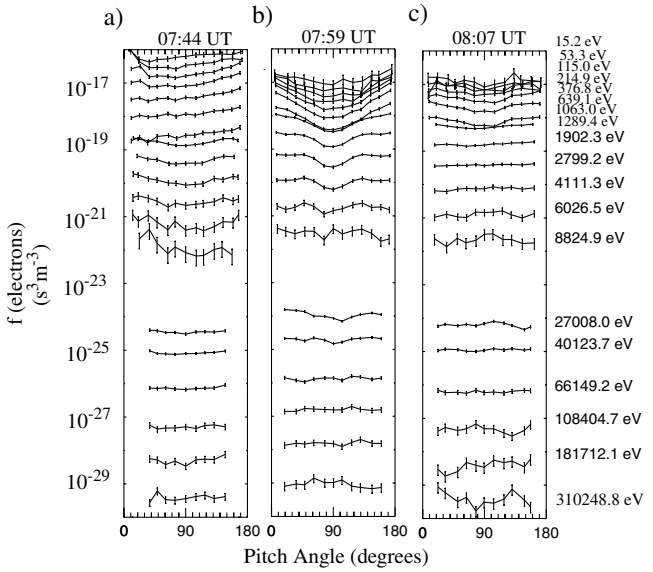

FIG. 4. Electron pitch angle distributions: (a) at 07:44 UT on the earthward side of the X line; (b) at 07:59 UT near the center of the diffusion region, at the peak of the energetic electron fluxes; (c) at 08:07 UT on the tailward side. The error bars show the maximum statistical error in the measurements.

The high-energy electron peak occurred at a time when the spacecraft encountered the neutral sheet [B_x close to zero in Fig. 1(c)]. However, the neutral sheet was also encountered outside the diffusion region, for example, at 09:35 UT [Fig. 1(c)], with no associated high-energy electron peaks. Thus, these two features do not appear to be related. Similarly, a local minimum in the magnetic field [Fig. 1(j)] coincided with the high-energy electron peak at the center of the diffusion region. However, local minima in the magnetic field magnitude are also observed outside the diffusion region (e.g., at 09:35 UT) with no enhancements of high-energy electrons.

Finally, lower hybrid wave turbulence [Fig. 1(k)] was seen intermittently throughout the interval of high speed flows and was not restricted to the diffusion region.

The observations just described are the first measurements of energetic particles inside a magnetic reconnection diffusion region. The observed energetic particle characteristics provide some clues to possible particle acceleration mechanisms. Below, we summarize the key observations and discuss candidate processes.

(1) The highest energetic electron fluxes and the hardest spectrum occur near the center of the diffusion region where the plasma jets originate. The flux level decreases monotonically away from the center of the diffusion region, suggesting that the electron energization occurs inside the diffusion region; the decrease in fluxes and softening of the spectrum outside suggest no further energization is taking place outside the diffusion region. Thus, at least for this event, we see no evidence for a

two-step process as proposed by Hoshino *et al.* [19], whereby the electrons are initially energized inside the diffusion region, and further energized in the outflow region. That proposal was made based on the observations of suprathermal (20–40 keV) electrons outside the diffusion region in the near-Earth (~ 30 Earth radii) magnetotail.

(2) The diffusion region electrons display strong field-aligned anisotropy at energies below 6 keV and gradually become isotropic with increasing energy. The observed symmetry between 0° and 180° fluxes throughout the diffusion region suggest closed field geometry on the earthward as well as tailward side of the reconnection site. This symmetry also suggests that, if parallel electric fields were responsible for electron acceleration, symmetric pairs of parallel fields, instead of unidirectional field, are required. Such field configurations have indeed been predicted in some simulations [25], although it is unclear how this field can accelerate electrons to 300 keV. Recent full particle simulations of 3D magnetic reconnection [26] show that electron holes are generated by the Buneman instability; these can lead to acceleration of electrons to relativistic velocities by the intense localized parallel electric fields in the diffusion region. However, to account for the observed isotropy of high-energy electrons, significant pitch-angle scattering would have to take place inside the diffusion region since acceleration by parallel electric fields is expected to result in strong field-aligned anisotropy in the electron distribution. The gradual flattening of pitch-angle spectra near 0° and 180° with increasing energy may be an indication of such scattering.

(3) In the event presented here, lower hybrid wave turbulence [27–29] was observed in the diffusion region, but these waves are also present outside the diffusion region and throughout the plasma sheet where high-energy electron fluxes are much lower. Thus, it is unclear whether these waves have any direct roles in the generation of the hundreds of keV electrons.

(4) The observed electron distribution at the center of the diffusion region is well approximated by a Maxwellian distribution with $N = 0.1\ \mathrm{cm}^{-3}$ and $T_e = 400$ eV for energies below ~2 keV and a power law function $f \propto E^{-4.8}$ for energies above 2 keV [Figs. 3(a) and 3(b)]. At the center of the diffusion region, the energy density contained in the electrons above 2 keV is $\sim 4\ \mathrm{eV\,cm}^{-3}$. The energy density of the Maxwellian portion of the distribution is $\sim 40\ \mathrm{eV\,cm}^{-3}$. By comparison, the kinetic energy density contained in the high speed plasma jets outside the diffusion region where the plasma velocity reaches $800\ \mathrm{km\,s}^{-1}$ is $\sim 700\ \mathrm{eV\,cm}^{-3}$. Although the amount of energy contained in the high-energy electron tail is a small fraction of the overall energy converted in reconnection, the reconnection diffusion region could still be a direct source of high-energy electrons commonly observed in the plasma sheet [16–18]. This conclusion is deduced from the fact that, during the 10 h of plasma sheet observations on this day, the highest flux of high-energy (> 12 keV) electrons was observed in the diffusion region.

We thank Adam Szabo for providing high resolution magnetic field data. We thank Jim McFadden, Chuck Carlson, and Masaki Fujimoto for helpful discussions. This research was funded in part by NASA Grant No. NAG5-10428 at U.C. Berkeley.

[1] E. R. Priest and T. Forbes, *Magnetic Reconnection: MHD Theory and Applications* (Cambridge University Press, Cambridge, England, 2000).
[2] R. G. Giovanelli, Nature (London) **158**, 81 (1946).
[3] V. M. Vasyliunas, Rev. Geophys. Space Phys. **13**, 303 (1975).
[4] E. R. Priest, in *Magnetic Reconnection in Space and Laboratory Plasmas* (American Geophysical Union, Washington, DC, 1984), p. 63.
[5] S. Tsuneta, Astrophys. J. **456**, 840 (1996).
[6] R. P. Lin and H. S. Hudson, Sol. Phys. **17**, 412 (1971).
[7] R. P. Lin, and H. S. Hudson, Sol. Phys. **50**, 153 (1976).
[8] G. Paschmann *et al.*, Nature (London) **282**, 243 (1979).
[9] R. L. McPherron *et al.*, J. Geophys. Res. **78**, 3131 (1973).
[10] T. Nagai, J. Geophys. Res. **106**, 25 929 (2001).
[11] B. U. Ö Sonnerup *et al.*, J. Geophys. Res. **86**, 10 049 (1981).
[12] J. T. Gosling *et al.*, J. Geophys. Res. **91**, 3029 (1986).
[13] T. D. Phan *et al.*, Nature (London) **404**, 848 (2000).
[14] C. M. Ho *et al.*, Geophys. Res. Lett. **21**, 3031 (1994).
[15] M. Øieroset *et al.*, J. Geophys. Res. **105**, 25 247 (2000).
[16] T. Terasawa and A. Nishida, Planet. Space Sci. **24**, 855 (1976).
[17] D. N. Baker and E. C. Stone, Geophys. Res. Lett. **3**, 557 (1976).
[18] D. N. Baker and E. C. Stone, J. Geophys. Res. **82**, 1532 (1977).
[19] M. Hoshino *et al.*, J. Geophys. Res. **106**, 25 979 (2001).
[20] M. Øieroset *et al.*, Nature (London) **412**, 414 (2001).
[21] F. Mozer, S. Bale, and T. D. Phan, Phys. Rev. Lett. **89**, 015002 (2002).
[22] J. D. Scudder *et al.*, J. Geophys. Res. (to be published).
[23] R. P. Lin *et al.*, Space Sci. Rev. **71**, 125 (1995).
[24] R. P. Lepping *et al.*, Space Sci. Rev. **71**, 207 (1995).
[25] P. L. Pritchett, J. Geophys. Res. **106**, 25 961 (2001).
[26] J. F. Drake *et al.*, APS Abstract **47**, 106 (2002).
[27] T. Okada *et al.*, Geophys. Res. Lett. **21**, 2931 (1994).
[28] C. Cattell *et al.*, Geophys. Res. Lett. **21**, 2987 (1994).
[29] I. Shinohara *et al.*, J. Geophys. Res. **103**, 20 365 (1998).
[30] B. U. Ö Sonnerup, in *Solar System Plasma Physics III*, edited by L. T. Lanzerotti, C. F. Kennel, and E. N. Parker (North-Holland, New York, 1979), p. 45.